IOP Conf. Series: Materials Science and Engineering **1344** (2026) 012063 doi:10.1088/1757-899X/1344/1/012063

Modelling two-phase He II flow for heat load limits in XFEL Cryomodules for CW operation

A K Dhillon*, S Barbanotti, Y Bozhko, K Jensch, R Ramalingam, E Abassi and T Schnautz

Deutsches Elektronen-Synchrotron DESY, Notkestr. 85, 22607 Hamburg, Germany

E-mail: aman.kumar.dhillon@desy.de

Abstract. The European XFEL (EuXFEL) is under consideration for a High Duty Cycle (HDC) upgrade to enhance the user's operational range by enabling short pulse, long pulse, and Continuous Wave (CW) operation. This will involve adding new CW-optimized Cryomodules (CMs) at the beginning of the EuXFEL linac, followed by existing CMs, which will need to handle higher 2 K dynamic heat loads. The key challenges for this upgrade are the design of the CW-optimized CMs and identifying the heat load limit of the existing EuXFEL CMs with respect to operational stability to meet the requirements of the HDC upgrade. Referring to operational stability, the flow conditions in the two-phase pipe of the CMs are crucial for a stable Radiofrequency (RF) operation. To address these challenges, a simulation model has been developed to analyze the two-phase flow behavior of superfluid helium in EuXFEL-like CMs at the Accelerator Module Test Facility (AMTF). This model incorporates the Taitel-Dukler criterion to evaluate the transitions in the two-phase pipe under varying heat loads. The findings provide path for the CW optimized CM design and JT valves arrangement, ensuring stable operation under increased heat loads. Validation tests at AMTF will confirm the model accuracy and support its application in XFEL HDC upgrade.

1 Introduction

The EuXFEL has been operational in Short Pulsed (SP) mode (burst mode) at 17.5 GeV with Duty Factor (DF) of around 1% since 2017 [1]. A proposed HDC upgrade aims to enable operation in CW mode with 100% DF or in Long Pulse (LP) mode with a DF ranging from 5% to 50% [2], offering an enhanced user operational range with improved beam stability [3].

Currently, the EuXFEL linac is subdivided and organized into three sections: L1, L2, and L3. These sections comprise 96 Cryomodules (CMs) that are arranged in nine strings, connected to each other by String Connection Boxes (SCBs). Most strings consist of 12 CMs, except for string 1 in L1 (4 CMs) and string 9 at the end of L3 (8 CMs).

For the HDC upgrade, the 16 CMs from L1 and L2 will be relocated to the end of L3. Of these, 4 CMs will extend the existing string 9 from 8 to 12 CMs. The remaining 12 CMs will form a new string 10 within L3. Consequently, strings 9 and 10 will be interconnected through a new SCB7 (see Figure 1). L1 and L2 will then be equipped with new CW optimized CMs, which must be designed to cope with a 2 K dynamic heat load of approximately 110 W each and a static heat load of approximately 10 W.

In the current operating mode (SP mode), the CMs in L3 experience a total heat load of approximately 13 W for each CM at 2 K (6.1 W static + 7.2 W dynamic), leading to a total heat load of 156 W for a nominal string with 12 CMs [4]. As per the string design, the maximum total heat load limit of a nominal string is 240 W, resulting in a heat load limit of 20 W per CM based on the current flow

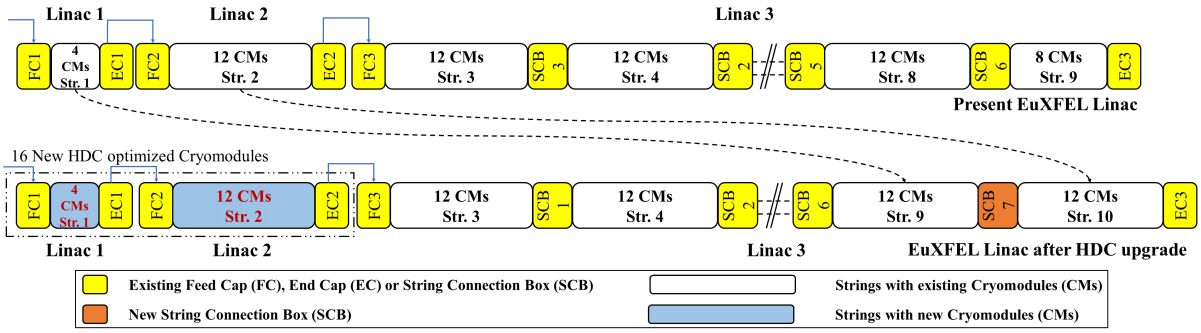

Figure 1. EuXFEL linac current and HDC upgrade configurations.

distribution [5]. In contrast, the total heat load of a nominal string in L3 is estimated to increase to approximately 384 W in CW operating mode. Consequently, it is essential to ensure that the existing CMs of EuXFEL are compatible with the upgrade, covering the increased 2 K heat loads of approximately 32 W per CM [6]. However, the design of existing CMs will not be modified. The only viable approach to effectively manage the increased heat load during LP and/or CW operation is to adjust the string design, implementing different flow distribution strategies of the 2 K supply by integrating additional JT valves in the strings of L3.

A significant challenge in evaluating the possibilities of operating the CMs in L3 with increased heat loads according to the different operating modes of the HDC upgrade is understanding the flow dynamics in the Two-Phase Pipe (2PP) of the CMs. Flow instabilities within this system can induce microphonic vibrations, potentially compromising stable cavity operation [5]. To mitigate this risk, a comprehensive investigation of two-phase flow dynamics is essential, focusing on critical parameters such as filling grade, vapor quality, and the positions of the JT valve as well as the Two-Phase Pipe and Gas Return Pipe (2PP-GRP) connection.

Therefore, extensive testing and validation of XFEL-like CMs on the cryomodule test stand in the Accelerator Module Test Facility (AMTF) is ongoing to identify operational limits when increasing 2 K dynamic heat loads. In this article, the simulation model has been applied to this configuration to understand the appearance of operational limits and the impact of parameters such as filling grade and vapor quality. Moreover, necessary design decisions can be taken, ensuring a stable and reliable performance of CMs organized in strings of L3 and operated under HDC conditions with increased 2 K dynamic heat loads.

2 Two-phase flow model

The 2 K system of the XFEL CM operates with a two-phase helium flow. The increased heat load from HDC operation will significantly alter the flow dynamics within the 2PP and may induce microphonic effects. This increased heat load can potentially cause undesirable instabilities. The transition from Stratified Smooth (SS) flow to Stratified Wavy (SW) flow which induces surface instabilities, is established as a critical limit for a stable two-phase operation [5].

A theoretical model has been developed to analyze this behavior to predict the transition between these flow regimes. The model is based on establishing velocity maps for LHe II and vapor inside the 2PP. Since the XFEL-like CMs themselves are not equipped with JT valves and 2PP-GRP connections, the velocity maps will depend on the arrangement of these components in a facility hosting the CMs for testing. The application of this model will be demonstrated on XFEL-like CMs horizontally installed on the cryomodule test stand in AMTF [7].

2.1 Flow distribution in 2PP of cryomodule

For a CM installed in AMTF, the JT valve and 2PP-GRP connection are placed on opposite sides of the 2PP. This results in a cocurrent flow of LHe II and vapor inside the 2PP, where the liquid and vapor flow in the same direction from the JT valve to the 2PP-GRP connection.

The two-phase flow in the XFEL CMs consists of saturated LHe II and vapor streams. As sub-cooled helium expands through the JT valve to 31 mbara, it produces flash gas that travels through the 2PP, collecting additional vapor from heat conducted by cavity chimneys. This vapor production increases stepwise with each chimney, leading to a corresponding decrease in liquid flow.

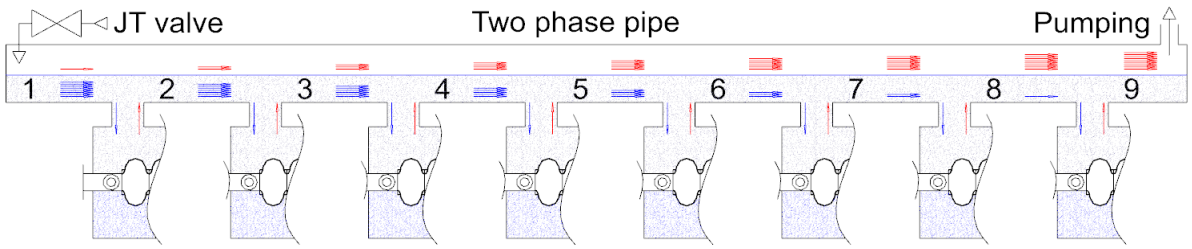

Figure 2. Flow map in the two-phase pipe of XFEL CMs installed at AMTF.

The 2PP can be subdivided into nine sections, each with variable liquid and vapor flow rates (Figure 2). The total heat load (Q) is spread evenly across eight cavities, leading to the LHe II mass flow rate $\dot{m}_L$ from the JT valve expressed as:

$$\dot{m}_L = \frac{Q}{h_{fg}} \tag{1}$$

where h_{fg} is the latent heat of He II.
The flash gas flow rate ($\dot{m}_G$) post-JT expansion is evaluated using quality factor (x)

$$\dot{m}_G = \dot{m}_L \cdot \frac{x}{1-x} \tag{2}$$

In the first section, liquid flow equals the full liquid mass flow from the JT valve, while subsequent sections experience a stepwise decrease in liquid flow and an increase in vapor flow. Specifically:

$$\left.\begin{array}{l}(\dot{m}_L)_n = \dot{m}_L\left(1-\frac{n-1}{8}\right)\\ (\dot{m}_G)_n = \dot{m}_G + \dot{m}_L \cdot \frac{n-1}{8}\end{array}\right\} \quad n = 1, 2, 3, \ldots, 8 \tag{3}$$

By the last section, the liquid remains stagnant and the vapor carries maximum flow due to upstream evaporation:

$$\left.\begin{array}{l}(\dot{m}_L)_9 = 0\\ (\dot{m}_G)_9 = \dot{m}_G + \dot{m}_L\end{array}\right\} \tag{4}$$

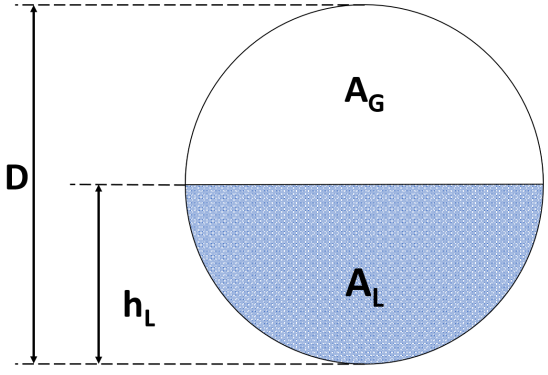

Figure 3. Schematics of two-phase flow in the 2PP.

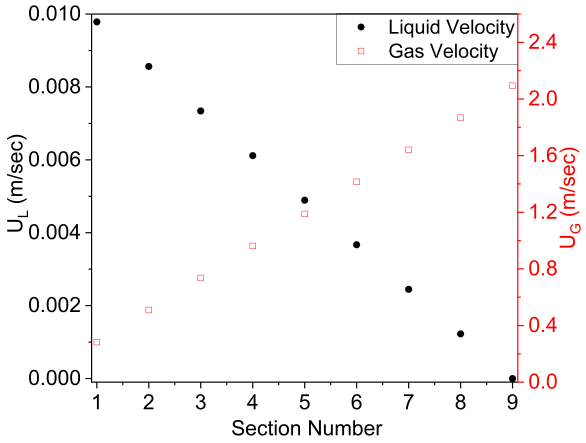

Figure 4. Linear velocity of liquid and vapor along the 2PP.

Denoting the cross-sectional areas of LHe II and vapor inside the 2PP as respectively A_L and A_G (Figure 3), the corresponding linear velocities of liquid U_L and vapor U_G can correspondingly be found as

$$U_L = \frac{\dot{m}_L}{A_L \cdot \rho_L} \tag{5}$$

$$U_G = \frac{\dot{m}_G}{A_G \cdot \rho_G} \tag{6}$$

where ρ_L and ρ_G are LHe II and vapor densities.

The distribution of flow rates of LHe II and vapor along the 2PP (flow maps) can be calculated at a heat load of 68.1 W using the eq. (5) and (6). These flow maps are converted into velocity maps (see Figure 4) for the 2PP (XFEL-like CMs) and assuming $A_L = A_G$ (i.e., the 2PP is filled to a half). This assumption remains valid along the entire pipe length because the liquid surface follows the Earth curvature while the pipe is installed horizontally, ensuring a constant liquid level. As a result, the liquid and vapor cross-sectional areas remain uniform throughout the pipe. One can observe that the LHe II velocities are of the order of several millimeters per second, while the vapor velocities are of the order of several meters per second.

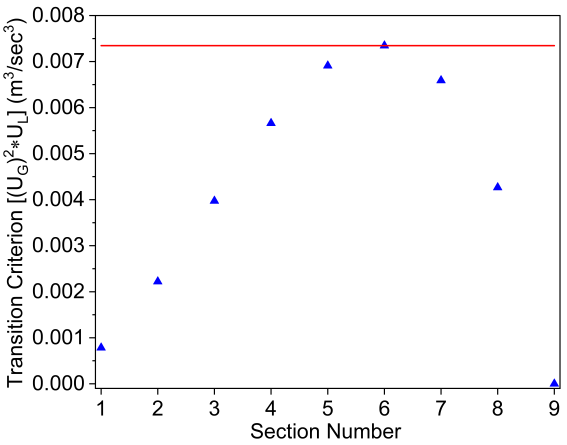

Figure 5. The $U_G^2 \cdot U_L$ factor along the 2PP.

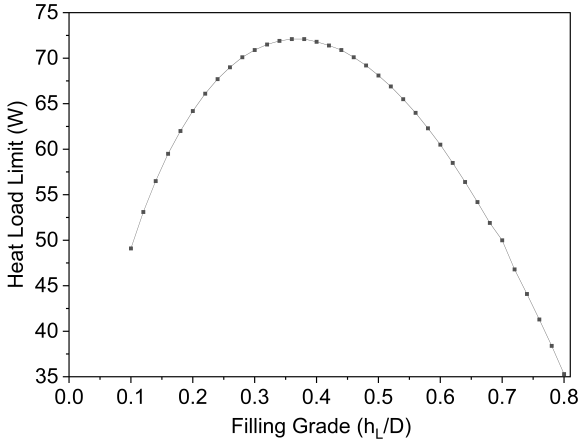

Figure 6. Influence of the filling grade on the heat load limit.

2.2 Transitional criteria for "stratified smooth - stratified wavy"

The criterion of the transition between the Stratified Smooth and Stratified Wavy (SS-SW) flow patterns based on the physical principles was developed by Taitel and Dukler [8]. According to this criterion, the linear velocity of gas should exceed a certain value defined as

$$U_G \geq \sqrt{4 \cdot \nu_L \cdot (\rho_L - \rho_G) \cdot \frac{g \cdot \cos(\alpha)}{\rho_G \cdot U_L \cdot s}} \tag{7}$$

where α is the inclination angle, ν_L is the kinematic viscosity of the liquid, g is the acceleration of gravity, and s is the correction factor, s=0.01.

Considering only a horizontal pipe and the 31 mbara operation, the wavy flow will then occur if

$$U_G^2 \cdot U_L \geq 0.007337 m^3/sec^3 \tag{8}$$

The obtained velocity map from Figure 4 can be converted into a $U_G^2 \cdot U_L$ factor flow map, as shown in Figure 5. As seen, the $U_G^2 \cdot U_L$ factor reaches the limiting value of 0.007337 m³/sec³ in section 6, i.e. the section 6 will transition into wavy flow. One can therefore conclude that the limiting heat load value for an XFEL-like CM installed at AMTF with the 2PP filled to a half will be ∼68.1 W for 31 mbara operation and the quality factor of x=0.135. The following sequence should then be applied for establishing the heat load limit for a CM:

- Assuming a guess value of the heat load
- Building a flow map in the 2PP considering the arrangement/number of JT valves and 2PP-GRP connections, and the quality factor
- Converting the flow map into a velocity one, considering the filling grade h_L/D, the 2PP internal diameter D, and the 2PP inclination

- Establishing the $U_G^2 \cdot U_L$ factors for all 2PP sections
- Checking whether the maximal value of the $U_G^2 \cdot U_L$ factor is equal to 0.007337 m^3/sec^3. If so, the guess value of the heat load is considered as the heat load limit. Otherwise, the guess value of the heat load should be readjusted and the whole sequence repeated.

The cross-sectional areas (A_L and A_G) depend on the filling grade of 2PP. The optimal value of the limiting heat load is achieved at a filling grade of approximately 37% [9]. Similarly, the limiting heat load can be evaluated for different filling grades in a horizontal 2PP featuring an inner diameter of 72.1 mm at a temperature of 2 K and a quality factor of $x = 0.135$. As shown in Figure 6, maintaining the filling grade within the specified range of 20% to 55% will ensure a maximum deviation of 10% from the maximum possible heat load limit. In the interest of methodological uniformity, all future calculations will consequently be performed at a filling grade of 50%.

2.2.1 Understanding of cos(α) for inclined CMs. The inclination angle α in eq. (7) refers to the angle between the pipe axis and the horizontal. In the case of inclined CMs, the inclination angle of the 2PP is not equal to that of the liquid-vapor interface.

Safe operation of the cavities in inclined CMs requires that LHe II covers at least the bottom edge of the 2PP at the uphill end, i.e., $h_L/D > 0$ at that location. In this state, all cavity chimneys are filled with LHe II, and the liquid surface inside the 2PP follows the Earth curvature. Consequently, the interface angle becomes effectively zero and independent of the pipe inclination.

Under these operational states, the terms "downhill flow" and "uphill flow" are not applicable – LHe II flows in the direction of LHe II consumers (chimneys). Thus, the installation position of the JT valve becomes irrelevant, provided its outlet is located above the 2PP and the connecting pipe between the JT valve outlet and the 2PP would not contain uphill parts to ensure only downhill flow.

While the inclination of the 2PP does not affect the interface angle in the operational state, it does influence the distribution of A_L and A_G along the 2PP. This should be taken into account when converting flow regime maps into velocity-based ones. Given the extremely small inclination angle of 2PP in the XFEL linac (0.14 milliradians), any vertical velocity component induced by gravity is negligible, and the bulk fluid velocity can be considered effectively horizontal.

2.3 Applicability of the SS-SW transition criterion for low LHe II velocities

It can be noted from Figure 4 that the 2PP has maximum vapor velocity in section 9. Under certain conditions, the application of SS-SW criterion may suggest that the stratified smooth flow can persist at very high vapor velocities with a correspondingly low liquid velocity. However, the stratified to non-stratified (S-NS) criterion, defined by Taitel-Duckler [8], may indicate a trainsition to a non-stratified flow regime under the same conditions.

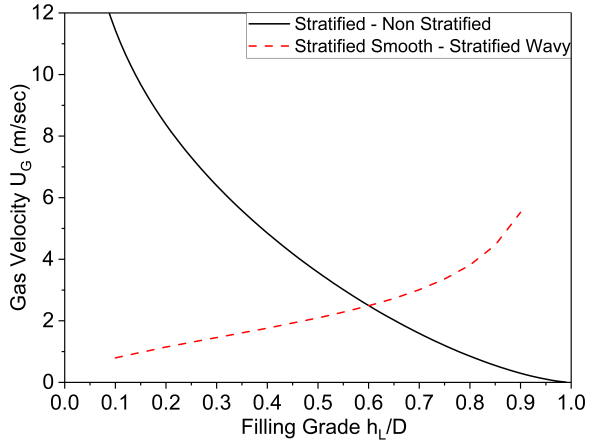

Figure 7. The vapor velocity in section 9 based on the SS-SW and S-NS criteria as a function of the filling grade.

According to Taitel-Duckler, the S-NS transition depends on the vapor velocity, and occurs when:

$$(U_G)^2 \geq \left(1 - \frac{h_L}{D}\right)^2 \cdot \frac{(\rho_L - \rho_G) \cdot g \cdot A_G}{\rho_G \cdot \left(\frac{\partial A_L}{\partial h_L}\right)} \qquad (9)$$

The corresponding LHe II velocity satisfying both the SS-SW criterion in eq. (7) and the S-NS criterion in eq. (9) can be expressed as:

$$U_L = \frac{400 \cdot \nu_L \cdot \left(\frac{\partial A_L}{\partial h_L}\right)}{A_G \cdot \left(1 - \frac{h_L}{D}\right)^2} \qquad (10)$$

A comparison of the two criteria is illustrated in Figure 7, which plots the vapor velocity U_G as a function of the filling grade h_L/D for a 2PP with a diameter $D = 72.1\ mm$. The black solid line represents the limiting vapor velocity in section 9 of the 2PP, calculated using the S–NS criterion (eq. (9)). The red dashed line corresponds to the vapor velocity in the same section when the $U_G^2 \cdot U_L$ product in section 6 equals 0.007337 m^3/sec^3, indicating the onset of stratified wavy flow as per eq. (7).

As shown, for filling grades above approximately 0.6, the SS–SW and S–NS criteria diverge in their classification of the flow regime. While the SS–SW criterion may still indicate stratified smooth flow, the S–NS criterion predicts a transition to non-stratified flow due to the dominance of vapor shear forces.

This disagreement arises because the SS–SW criterion focuses on surface instabilities that cause wave formation on the liquid interface, whereas the S–NS criterion considers bulk momentum effects that disrupt the stratified structure entirely [8].

When such conflicting assessments occur particularly during calculations of limiting heat load, it seems more appropriate to adopt the S–NS criterion. This is because the onset of non-stratified flow typically leads to more significant changes in flow dynamics, such as increased turbulence, pressure drop, and phase interaction, all of which critically influence the thermal and hydraulic performance of the system.

2.4 Analytical Solution

Assuming that the total heat load is evenly distributed along the entire length of the 2PP, the liquid flow rate at the end of pipe opposite to the JT valve will be equal to zero. Further assuming the pipe length is equal to unity, the function describing the dependence of the liquid and gas flow rate as a function of the distance l from the JT valve are given by:

$$\dot{m}_L(l) = \frac{Q \cdot (1-l)}{h_{fg}} \tag{11}$$

$$\dot{m}_G(l) = \frac{Q}{h_{fg}} \cdot \left[\frac{1}{1-x} - (1-l)\right] \tag{12}$$

Correspondingly, the dependence of the linear velocity on distance l is defined as:

$$U_L(l) = \frac{Q \cdot (1-l)}{h_{fg} \cdot A_L \cdot \rho_L} \tag{13}$$

$$U_G(l) = \frac{Q}{h_{fg} \cdot A_G \cdot \rho_G} \cdot \left[\frac{1}{1-x} - (1-l)\right] \tag{14}$$

The factor defining the transition to wavy flow, according to eq. (8), is:

$$[U_G(l)]^2 \cdot U_L(l) = \frac{Q^3}{h_{fg}^3 \cdot A_G^2 \cdot A_L \cdot \rho_L \cdot \rho_G^2} \cdot (1-l) \cdot \left[\frac{1}{1-x} - (1-l)\right]^2 \tag{15}$$

The maximum value of the function $f = (1-l) \cdot \left[\frac{1}{1-x} - (1-l)\right]^2$ in eq. (15) can be determinded by differentiating it with respect to the distance l, and setting the derivative equal to zero. The resulting equation defines the critical length l_{crit}, at which the transition to wavy flow first occurs, as a function of the quality x:

$$l_{crit} = 1 - \frac{1}{3(1-x)} \tag{16}$$

This equation is valid for $x \leq \frac{2}{3}$. For $x > \frac{2}{3}$, the critical length will always be zero, $l_{crit} = 0$, i.e., the transition to wavy flow takes place in the immediate vicinity of the JT valve.

By substituting eq. (16) into eq. (15), and equating the right-hand side of eq. (15) to 0.007337 $\mathrm{m}^3/\mathrm{sec}^3$, one can derive the dependence of the limiting heat load on the 2PP diameter D and quality x, under the condition $A_L = A_G$:

$$Q_{lim}\ [W] = 0.015 \cdot (1-x) \cdot (D\ [mm])^2 \tag{17}$$

The limiting heat load Q_{lim} and critical length l_{crit}, calculated using eq. (17) and (16), are amounted to be 67.4 W and 0.61, respectively, for the quality $x = 0.135$ and diameter $D = 72.1\ mm$. When the quality is increased to $x = 0.45$, Q_{lim} decreases to 42.9 W and l_{crit} to 0.39.

The vapor quality downstream of the JT expansion plays a critical role in determining the limiting heat load in the 2PP, as it governs the amount of flash gas generated. When the JT valve and the 2PP-GRP connection are placed on opposite sides, the flash gas must travel the full length of the 2PP, making the heat load highly sensitive to variations in quality. This behavior is influenced by the JT heat exchanger performance.

A minor discrepancy in the values of the limiting heat load Q_{lim} obtained using the analytical prediction ($\sim$67.4 W) and the computational model ($\sim$68.1 W) is attributed to the fact that the analytical prediction assumes a linear distribution of the heat load, whereas the computational model is based on a discrete one.

3 Heat load limit for XFEL like cryomodule

For a certain heat load, the linear velocities of liquid and vapor are evaluated across each section of the 2PP. The local flow regime transitions in these sections are identified using the SS-SW criteria (eq. (7)) for the onset of wavy flow and the S-NS criterion (eq. (9)) for the transition to non-stratified flow.

The first appearance of wavy flow occurs in section 6 at a heat load of $\sim$68.1 W, assuming a small quantity of flash gas (x =0.135), which is typical for test facilities equipped with a JT heat exchanger. However, the appearance of the wavy flow in a single section of the 2PP may not necessarily prohibit a stable Radiofrequency (RF) operation. The operational stability becomes more sensitive when several sections simultaneously experience the wavy flow.

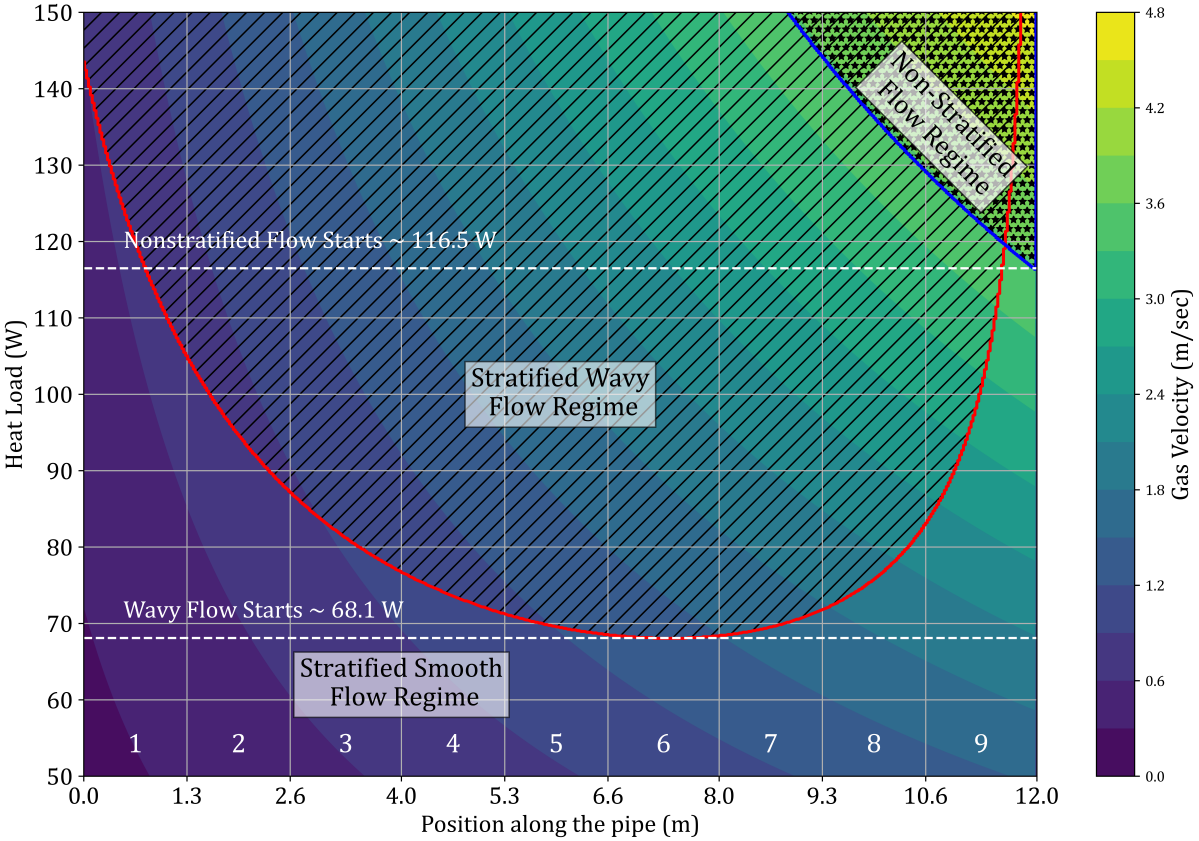

Figure 8. Dependence of the limiting heat load on the number of 2PP sections exhibiting stratified wavy or non-stratified flow regimes. The red bordered line shaded region indicates the flow regime defined by the SS–SW criterion. The blue bordered star shaded region indicated the flow regime defined by the S–NS criterion ($D = 72.1mm, h_L/D = 0.5, x = 0.135$).

Figure 8 shows the dependence of the heat load limit on a number of sections with shaded flow regimes. As the heat load increases, the region of stratified wavy flow expands along the 2PP. Notably, at a heat load of $\sim$75 W, the wavy flow is already present in 4 sections of the 2PP (roughly half of the 2PP length). The onset of wavy flow occurs gradually along the pipe, section by section, as the heat load increases. This progression follows the SS–SW criterion applied locally in each section and is clearly illustrated in Figure 8. This criterion effectively captures the dynamic transition from stratified smooth to wavy flow.

Beyond the 116.5 W threshold, a transition to non-stratified flow occurs, which is marked in the plot by the upper dashed line. This regime involves more intense phase interaction, greater turbulence, and reduced interface stability, which significantly raises the risk of RF performance degradation.

4 Conclusion

The present work introduces a comprehensive simulation model developed to analyze two-phase He II flow within the 2PP of EuXFEL CMs, particularly in relation to the upcoming HDC upgrade. Utilizing the Taitel-Dukler criteria, the model effectively captures the transition from stratified smooth to stratified wavy and stratified to non-stratified flow under varying operational conditions, offering valuable insights into flow stability and its possible effects on the RF operation in CM.

The investigation into the heat load limits for XFEL-like CMs at AMTF reveals critical dependencies on various parameters, including inclination, filling grade, number and arrangement of JT valves and 2PP-GRP connections, the 2PP diameter and helium quality. The analysis demonstrates that the emergence of wavy flow ($\sim$68.1 W) and non-stratified flow ($\sim$116.5 W) significantly correlates with the heat load, with specific thresholds identified for the onset of these flow regime. Maintaining stratified smooth flow in the 2PP might be critical for stable RF operation. Widespread wavy or non-stratified flow, driven by high heat loads or vapor quality, can compromise thermal stability.

In addition to validating analytical predictions, the model will serve as a crucial tool for defining the configuration of CW-optimized CMs and the layout of JT valves in L3 to meet the operational demands of the HDC upgrade. Therefore, a series of planned testes at AMTF will provide experimental validation, reinforcing the reliability of the model.

5 Recommendations

To maintain the $U_G^2 \cdot U_L$ factor below the stratified smooth–stratified wavy (SS–SW) transition limit, the following approaches are recommended:

- **Optimized Arrangement of JT valves and 2PP-GRP Connections:** Placing the JT valve and the 2PP-GRP connection on the same side significantly reduces the limiting heat load such as from 68.1 W to about 41 W at AMTF.
- **Increasing the Internal Diameter of the 2PP:** A larger internal diameter decreases the linear velocities of LHe II and vapor, helping to maintain a more stable two-phase flow regime.
- **Increasing the Number of JT valves per 2PP:** Adding more JT valves reduces the linear velocities of LHe II and flash gas, though it makes liquid level control more challenging. Alternatively, a single JT valve with multiple outlets can be considered.
- **Increasing the Number of 2PP-GRP Connections:** Multiple aligned 2PP-GRP connections minimize boil-off gas velocity, allowing for a limiting heat load of approximately $\sim$155 W in a half-filled 2PP with D=72.1 mm, compared to $\sim$67.4 W with a single connection.

These recommendations are vital to suppress wavy flow along the 2PP and avoid transition to non-stratified regimes, which heighten interfacial turbulence and risk RF performance. When SS–SW and S–NS criteria diverge (especially at higher filling grades), design choices should prioritize the S–NS threshold, since non-stratified flow is the more critical limit for thermal and hydraulic stability.

References

[1] Barbanotti S *et al.* 2024 *IOP Conference Series: Materials Science and Engineering* **1301** 012097 ISSN 1757-899X

[2] Bellandi A *et al.* 2023 *Frontiers in Physics* **11** 1–7 ISSN 2296424X

[3] Brinkmann R *et al.* 2014 *Nuclear Instruments and Methods in Physics Research Section A: Accelerators, Spectrometers, Detectors and Associated Equipment* **768** 20–25 ISSN 0168-9002 (*Preprint* 1403.0465)

[4] Ramalingam R *et al.* 2022 *IOP Conference Series: Materials Science and Engineering* **1240** 012123 ISSN 1757-899X

[5] Gubarev V *et al.* 2008 *AIP Conference Proceedings* **985** 1602–1609 ISSN 0094243X

[6] Sekutowicz J *et al.* 2013 Feasibility of CW and LP operation of the XFEL LINAC *Proceedings of FEL2013* (New York, NY, USA) pp 189–192 ISBN 9783954501267

[7] Bozhko Y *et al.* 2010 Cryogenics of European XFEL Accelerator Module Test Facility *Proceedings of ICEC23, Wroclaw* pp 911–918

[8] Taitel Y and Dukler A E 1976 *International Journal of Multiphase Flow* **2** 591–595 ISSN 03019322

[9] Xiang Y *et al.* 2000 *IEEE Transactions on Applied Superconductivity* **10** 1530–1533 ISSN 10518223